International Journal of Pharmaceutics 358 (2008) 168–176

Contents lists available at ScienceDirect

International Journal of Pharmaceutics

journal homepage: www.elsevier.com/locate/ijpharm

Activity of a sodium-dependent vitamin C transporter (SVCT) in MDCK-MDR1 cells and mechanism of ascorbate uptake

Shuanghui Luo, Zhiying Wang, Viral Kansara, Dhananjay Pal, Ashim. K. Mitra*

Division of Pharmaceutical Science, School of Pharmacy, University of Missouri-Kansas City, 5005 Rockhill Road, Kansas City, MO 64110-2499, USA

ARTICLE INFO

Article history:
Received 20 November 2007
Received in revised form 27 February 2008
Accepted 3 March 2008
Available online 13 March 2008

Keywords:
Ascorbic acid (AA)
SVCT
Uptake and transport
Substrate specificity
Regulation
MDCK-MDR1

ABSTRACT

The objective of this research was to functionally characterize sodium-dependent vitamin C transporter (SVCT) in MDCK-MDR1 cells and to study the effect of substituted benzene derivatives on the intracellular accumulation of ascorbic acid (AA). Mechanism of AA uptake and transport was delineated. Uptake of [^{14}C]ascorbic acid ([^{14}C]AA) was studied in the absence and presence of excess unlabelled AA, anion transporter inhibitors, and a series of mono- and di-substituted benzenes. Transepithelial transport of [^{14}C]AA across polarized cell membrane has been studied for the first time. Role of cellular protein kinase-mediated pathways on the regulation of AA uptake has been investigated. The cellular localizations of SVCTs were observed using confocal microscopy.

Uptake of AA was found to be saturable with a K_m of 83.2 μM and V_{max} of 94.2 pmol/min/mg protein for SVCT1. The process was pH, sodium, temperature, and energy-dependent. It was under the regulation of cellular protein kinase C (PKC) and Ca^{2+}/CaM mediated pathways. [^{14}C]AA uptake was significantly inhibited in the presence of excess unlabelled AA and a series of electron-withdrawing group, i.e., halogen- and nitro-substituted benzene derivatives. AA appears to translocate across polarized cell membrane from apical to basal side (A–B) as well as basal to apical side (B–A) at a similar permeability. It appears that SVCT1 was mainly expressed on the apical side and SVCT2 may be located on both apical and basal sides. In conclusion, SVCT has been functionally characterized in MDCK-MDR1 cells. The interference of a series of electrophile-substituted benzenes on the AA uptake process may be explained by their structural similarity. SVCT may be targeted to facilitate the delivery of drugs with low bioavailability by conjugating with AA and its structural analogs. MDCK-MDR1 cell line may be utilized as an *in vitro* model to study the permeability of AA conjugated prodrugs.

1. Introduction

Ascorbic acid (AA, vitamin C) is an essential nutrient required for mammalian cell growth, function, and wound healing. It serves as an antioxidant agent and plays essential role in the defense against free radicals (Rose, 1988; Wilson, 2005). Some mammals, i.e., man, primates, pigs and flying mammals cannot synthesize AA and must absorb it from diet by intestine; others can synthesize AA in the liver. AA is obtained for human body by the intestinal absorption from exogenous sources. Kidney maintains the balanced plasma level of this vitamin by reabsorption, filtration and excretion. Uptake of AA has been studied in cell types from various organs such as intestine (Maulen et al., 2003; Said and Mohammed, 2006), kidney (Bowers-Komro and McCormick, 1991; Rose, 1986), brain (Astuya et al., 2005; Castro et al., 2001), eye (Garland, 1991; Talluri et al., 2006), bone (Dixon et al., 1991), and skin (Padh and Aleo, 1987).

A transport system is necessary to deliver AA to various tissue cells. Recently, two isoforms of sodium-dependent vitamin C transporters, SVCT1 and SVCT2, have been cloned from human and rat DNA libraries (Daruwala et al., 1999; Tsukaguchi et al., 1999; Wang et al., 1999). Both SVCT carriers have similar functions and can mediate L-AA transport with high affinity. SVCT1 is mainly expressed in epithelial cells of kidney, intestine, and liver, whereas SVCT2 is widely distributed in brain, eye, and other organs (Tsukaguchi et al., 1999). Residence of SVCT1 in apical cell surface in polarized cell membrane has been reported in both Caco-2 and MDCK cells by functional and confocal imaging studies (Boyer et al., 2005; Maulen et al., 2003; Subramanian et al., 2004).

Substrate specificity of SVCT has been probed in several recent works. Dixon and co-workers studied ascorbate uptake by osteoblast cells and found that uptake of ascorbate was reversibly inhibited by antagonists of anion transporter such as 4,4′-diisothiocyanostilbene 2,2′-disulfonic acid (DIDS), 4-acetamido-4′-isothiocyanostilbene-2,2′-disulfonic acid (SITS), sulfinpyrazone and furosemide, but not inhibited by organic anions, i.e., formate, lactate, gluconate, succinate except salicylate (Dixon et al., 1991).

* Corresponding author. Tel.: +1 816 235 1615; fax: +1 816 235 5190.
E-mail address: mitraa@umkc.edu (Ashim.K. Mitra).

0378-5173/$ – see front matter © 2008 Elsevier B.V. All rights reserved.
doi:10.1016/j.ijpharm.2008.03.002

It was concluded that ascorbate transporter is relatively specific for ascorbate and anion inhibitors interacted directly with ascorbate transporter. At pH 7.4, AA exists in the deprotoned form as an anion (−1 value). Therefore, it is not surprising that AA uptake was inhibited by anion inhibitors. To better understand the substrate specificity of SVCT, Rumsey and colleagues studied the inhibition of AA analogs by human skin fibroblast cells and demonstrated that a series of 6-halo-6-deoxy-L-AA were the most effective compounds to inhibit AA uptake (Rumsey et al., 1999). This study reported that the structural specificity requirement of ascorbate analogs to be an inhibitor was a C-4S absolute configuration in a five-membered reduced ring with no substitution on carbon 2 or 3. Later on, Park and Levine (2000) reported that flavonoids inhibited the uptake of both AA and dehydro-AA due to their structural similarity. More recently, Dalpiaz and his group demonstrated the inhibition of diclofenamic acid to the AA uptake in human retinal pigment epithelium cells while studying the properties of AA conjugates of nipecotic acid, kynurenic acid, and diclofenamic acid (Dalpiaz et al., 2004, 2005a,b; Manfredini et al., 2004). Significant lowering in AA uptake by 6-halo-deoxy-AA and diclofenamic acid in different cells suggested that the substrate specificity of SVCT is relative and halogen-substituted benzene may affect AA uptake. To test this hypothesis, we studied the effect of a series of mono- and di-substituted benzenes on the uptake of AA in MDCK-MDR1 cells.

MDCK-MDR1 cell line is derived from Madin–Darby canine kidney cells which were transfected with the human MDR1 gene. These cells express high levels of P-gp and differentiate rapidly. This cell line has been utilized as an alternative to Caco-2 model for high throughput screening of permeability and drug–drug interactions in drug discovery (Tang et al., 2002). It has also been employed in our laboratory to study the permeability of nutrient conjugated prodrugs of saquinavir (Jain et al., 2005; Luo et al., 2006). To establish the utility of MDCK-MDR1 cell line as an *in vitro* model for uptake and transport of AA conjugated prodrugs of protease inhibitors, we attempted to delineate the mechanism of AA uptake and transport in MDCK-MDR1 cells.

2. Materials and methods

2.1. Materials

[^{14}C]ascorbic acid ([^{14}C]AA, 8.5 mCi/mmol) was procured from PerkinElmer Life Science, Inc. (Boston, MA). Unlabelled AA; substituted benzene derivatives including chlorobenzene, bromobenzene nitrobenzene, phenol, benzaldehyde, benzoic acid, 4-chlorophenol, 4-bromophenol, 4-iodophenol, 4-nitrophenol, 4-chloroaniline, 4-bromoaniline, 1,4-di-iodobenzene, and 4-iodoanisole; anion transporter inhibitors including DIDS, SITS, probenecid and para amino hippuric acid (PAHA); metabolic inhibitors, i.e., 2,4-dinitrophenol (DNP), sodium azide (NaN_3), and ouabain were purchased from Sigma–Aldrich Co. (St. Louis, MO). Dithiothreitol (DTT), choline chloride, potassium phosphate, and various modulators of cellular signaling pathways, i.e., calmidazolium, 1-[*N*,*O*-bis(5-isoquinolinesulfonyl)-*N*-methyl-L-tyrosyl]-4-phenylpiperazine (KN-62), phorbol 12-myristate 13 acetate (PMA), H-89, forskolin and all other reagents were also obtained from Sigma–Aldrich. MDCK-MDR1 cells were donated by P. Borst (Netherlands Cancer Institute, Amsterdam, The Netherlands). The growth medium, Dulbecco modified Eagle medium (DMEM), nonessential amino acids (NEAA), calf serum (CS), and trypsin/EDTA were obtained from Gibco (Invitrogen, Grand Island, NY). Penicillin, streptomycin, sodium bicarbonate, and HEPES were purchased from Sigma–Aldrich. Dulbecco modified phosphate buffer saline (DPBS) was prepared with 129 mM NaCl, 2.5 mM KCl, 7.4 mM Na_2HPO_4, 1.3 mM KH_2PO_4, 1 mM $CaCl_2$, 0.7 mM $MgSO_4$, and 5.3 mM glucose at pH 7.4. DPBS also contained 20 mM HEPES. These chemicals were of analytical grade, obtained from Sigma–Aldrich. Culture flasks (75 cm^2 growth area), Polyester Transwell® (pore size of 0.4 μM and 12 mm diameter) and 12-well tissue culture plates were purchased from Costar (Cambridge, MA).

2.2. Cell culture

MDCK-MDR1 cells (passages 5–15) were cultured in DMEM supplemented with 10% calf serum (heat inactivated), 1% nonessential amino acids, 100 units/mL penicillin, 100 g/mL streptomycin, 25 mM HEPES, and 29 mM sodium bicarbonate at pH 7.4. Cells were allowed to grow at 37 °C in a tissue culture incubator with 5% CO_2 and 95% air for 3–4 days to reach 80% confluence, and then were plated at a density of 66,000 cm^{-2} in 12-well tissue culture plates. Cells were then incubated at 37 °C in a humidified atmosphere of 5% CO_2 and 95% air and grown for 6–7 days to reach confluence. The medium was changed every other day.

2.3. Uptake studies

2.3.1. General procedure of uptake experiments

Uptake studies were conducted with confluent cells. The medium was removed and cells were rinsed three times, 10 min each with 2 mL of DPBS buffer at 37 °C, unless otherwise stated. In a typical uptake experiment, cells were incubated with 1 mL of [^{14}C]AA solution with/without predefined unlabelled chemicals (AA, a series of substituted benzene derivatives and anion transporter inhibitors) prepared in DPBS (pH 7.4) at 37 °C for 30 min, except for time course studies. This time period remained within linear range. In all the experiments, 0.5 mM DTT was added to prevent any oxidation of AA. After the incubation period, the cell monolayer was rinsed three times with ice-cold stop solution (200 mM KCl and 2 mM HEPES) to terminate drug uptake. Cells were left overnight in 1 mL lysis solution [0.1% (v/v) Triton X-100 in 0.3 N NaOH] at room temperature. Aliquots (500 μL) from each well were then transferred to scintillation vials containing 5 mL scintillation cocktail (Fisher Scientific, Fairlawn, NJ). Samples were analyzed using liquid scintillation counter (Model LS-6500, Beckman Instruments, Inc., Fullerton, CA). The rate of uptake was normalized to the protein content of each well. Amount of protein in the cell lysate was measured by a BioRad protein estimation kit (BioRad, Hercules, CA).

2.3.2. Na^+ dependency

To study Na^+ dependency, sodium chloride and sodium phosphate in the incubation media were replaced by equimolar choline chloride and potassium phosphate, to generate sodium free medium.

2.3.3. pH dependency

Incubation media were adjusted at different pHs (5.0, 6.0, 6.5, 7.4, 8.5) by adding 1 N HCl or NaOH. Cells were rinsed with DPBS of different pH values. Permeant solutions ([^{14}C]AA) were also prepared in DPBS at these pH values.

2.3.4. Energy dependency

To determine whether the uptake of [^{14}C]AA is energy-dependent, we also examined the effect of metabolic inhibitors, i.e., DNP, NaN_3, and ouabain (all at the concentration of 1 mM) on the uptake process. Three different methods were employed: After rinsing the cells with DPBS buffer 3 mm × 10 min, (1) preincubating the cells with solutions of metabolic inhibitors for 30 min, (2) simultaneously incubating the uptake of AA with the metabolic inhibitors for 30 min, and (3) preincubating the cells for 10 min and followed

by inhibiting the uptake process with the metabolic inhibitors for 30 min.

2.3.5. Concentration dependency

Various concentrations (5–500 μM) of unlabelled AA solutions were prepared in DPBS. [^{14}C]AA (23.5 μM) was added to each tube containing various concentrations of unlabelled AA to prepare donor solutions. Then, the uptake of AA was carried out. The data was fitted to a Michaelis–Menten equation as shown in Section 2.6 and the apparent affinity constant K_m and maximum uptake velocity V_{max} of sodium-dependent AA uptake were determined.

2.3.6. Substrate specificity of SVCT

[^{14}C]AA uptake was carried out in the absence and presence of 1 mM unlabelled AA, anion transporter inhibitors including DIDS, SITS, probenecid and PAHA, and a series of mono- and di-substituted benzene derivatives including chlorobenzene, bromobenzene nitrobenzene, phenol, benzaldehyde, benzoic acid, 4-chlorophenol, 4-bromophenol, 4-iodophenol, 4-nitrophenol, 4-chloroaniline, 4-bromoaniline, 1,4-di-iodobenzene, and 4-iodoanisole.

2.3.7. Regulation of cellular protein kinase-mediated pathways

In order to investigate the regulation of intracellular protein kinase-mediated pathways involved in AA uptake, cells were preincubated with various modulators of cellular signaling pathways, i.e., calmidazolium (50 μM) and KN-62 (10 μM), inhibitors of Ca^{2+}/calmodium pathway; PMA (5 μM), an activator of PKC; H-89 (25 μM) and forskolin (100 μM), simulators of PKA-mediated pathway, respectively. Uptake experiments were performed according to a method described in Section 2.3.1.

2.4. Transepithelial transport

Permeability of [^{14}C]AA (23.5 μM) across MDCK-MDR1 cell monolayers was determined using 12-well Transwell® plates. Before each experiment, cells were grown on Transwell® inserts (diameter 12 mm) for 6–7 days. Medium was aspirated and cell monolayers were rinsed three times (10 min each wash) with DPBS pH 7.4 at 37 °C. Volumes of apical and basal chambers were 0.5 and 1.5 mL, respectively. Transport experiments were conducted for a period of 3 h. Aliquots (100 μL) were withdrawn from the receiver chamber at predetermined time intervals, i.e., 15, 30, 45, 60, 90, 120, and 180 min and replaced with fresh DPBS buffer to maintain sink conditions. Dilutions were taken into account for the calculations. Samples were added to 5 mL scintillation cocktail and then analyzed by scintillation counter (Model LS-6500, Beckman Instruments, Inc.). All transport experiments were performed at 37 °C.

2.5. Confocal microscopic imaging

The polar locations of SVCT1 and SVCT2 were determined by *fluorescence imaging* using confocal microscope. After MDCK-MDR1 cells were grown on Transwell® inserts for 6–7 days, rinsed with PBS for three times and then fixed in freshly made cold 4% paraformaldehyde in PBS for 20 min at 4 °C. The cells were rinsed with cold PBS for four times. To increase the cellular permeability of antibodies across cellular membrane, the cells were treated with ascending grade of ethanol 50% (2 min), 70% (2 min), 95% (5 min), and then back to descending grade of ethanol with 70% (1 min), 50% (1 min) and PBS. The cells were incubated with a solution of 1% BSA and 4% non-fat dry milk in PBS for non-specific binding for 1 h at room temperature (RT). The cells were rinsed with PBS again, and then incubated with goat polyclonal primary antibodies (Santa Cruz) for SVCT1 and SVCT2 (diluted 1:50 as per manufacture's instruction) separately for 2 h at 37 °C. The goat serum was used as control. Then the cells were washed with PBST for three times 15 min each at RT. The cells were exposed to anti-goat Ig-G–FITC secondary antibodies (diluted 1:200 as per Sigma's instruction) at 37 °C for 1 h. The cells were washed with PBST for four times (15 min each) at RT. The plates were covered with foil to avoid light. The membranes were cut along the edges, placed on the glass slides, and covered with cover glasses using mounting medium. The slide box was kept in the refrigerator until observed and pictured using confocal fluorescence microscopy. Z-stack pictures were taken from top to bottom. The fluorescence localized on the apical side of the cells cannot be seen in the bottom picture. However, if the fluorescence localized in the bottom side of the cells can be visualized in all Z-stack pictures.

2.6. Data analysis

Kinetic parameters of AA uptake were calculated with a computer program KaleidaGraph 3.5. The data was plotted and fitted to a Michaelis–Menten equation (Eq. (1)) and the parameters K_m and V_{max} were obtained.

$$v = \frac{V_{max}[C]}{K_m + [C]} \quad (1)$$

v is the initial uptake rate, V_{max} is the maximal velocity, K_m is Michaelis–Menten constant, and C is the total concentration of both radiolabeled and unlabelled AA.

The cumulative amount of [^{14}C]AA transported is calculated by Eq. (2)

$$TR_{cum} = A_n + \frac{VS_n}{V_r}\sum_{i=0}^{n-1} A_i \quad (2)$$

A_n is the amount of AA measured in sample n, VS_n is the volume of sample n, V_r is the volume of the receiver chamber, and A_i is the amount of AA at each predetermined time point.

Transepithelial transport permeability P (P_{A-B} or P_{B-A}) of [^{14}C]AA was calculated according to Eq. (3):

$$P = \left(\frac{d(TR_{cum})}{dt}\right) \times \frac{1}{A} \times \frac{1}{C_0} \quad (3)$$

$d(TR_{cum})/dt$ is transport rate, which was obtained from the slope of the cumulative amount (TR_{cum}) – time profile. A is the surface area of the Transwell® insert, and C_0 is the donor concentration. Values are expressed as centimeters per second.

2.7. Statistical analysis

All experiments were conducted at least in triplicate and results were expressed as mean ± S.D. Statistical comparisons of mean values were evaluated by Student's t-test using GraphPad InStat version 3.1 (GraphPad). $P < 0.05$ was considered to be significant.

3. Results

3.1. Time course

Figure 1 depicts the time course of the intracellular accumulation of AA in MDCK-MDR1 cells at 37 °C. Uptake was linear for up to 90 min of incubation time ($r^2 = 0.996$) and occurred at the rate of 9.82 pmol/min/mg protein. An incubation period of 30 min was selected for subsequent uptake experiments unless otherwise mentioned.

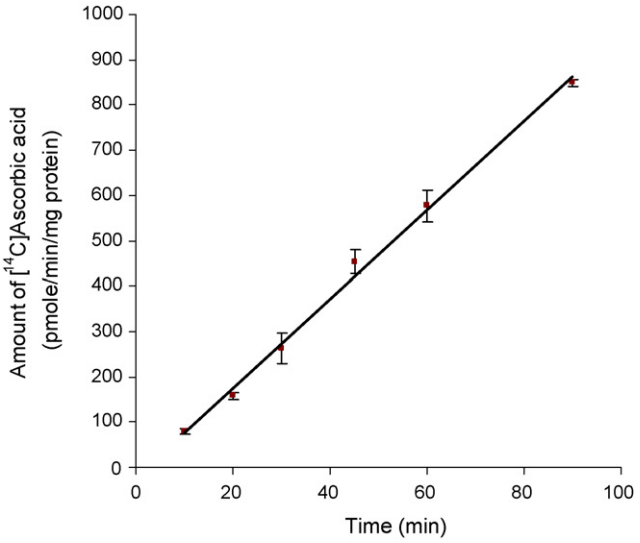

Fig. 1. Time course of [^{14}C]AA uptake in MDCK-MDR1 cells. Uptake of [^{14}C]ascorbic acid ([^{14}C]AA, 0.2 μCi/mL, 23.5 μM) was measured in DPBS buffer (pH 7.4) at 37 °C. Data is shown as mean ± S.D., n = 3–6. S.D. means standard derivation. When not shown, error bar is smaller than symbol. The linear equation is: $y = 9.82x - 20.72$ ($r^2 = 0.996$).

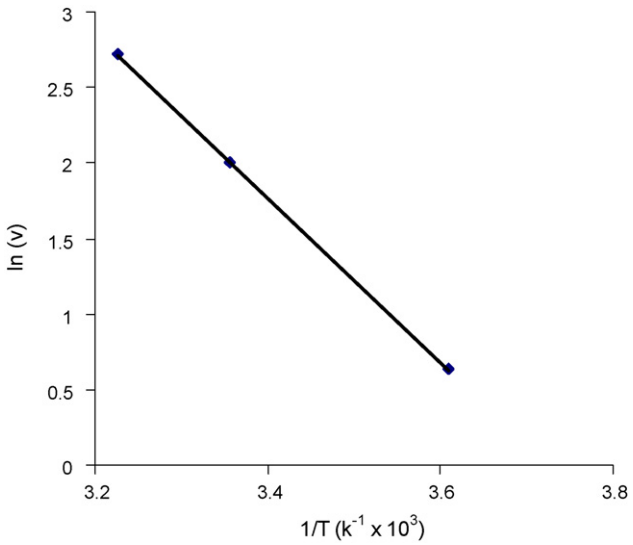

Fig. 3. Arrhenius plot of the effect of temperature on [^{14}C]AA uptake in MDCK-MDR1 cells. Uptake of [^{14}C]AA (23.5 μM) was measured in DPBS buffer (pH 7.4) for 30 min at 37, 25 and 4 °C, respectively. Data is shown as mean ± S.D., n = 4–6.

3.2. Sodium dependency

The initial uptake rates of AA were found to be 19.6 ± 0.11 and 1.05 ± 0.054 pmol/min/mg protein in the presence and absence of sodium, respectively (Fig. 2). Replacing Na^+ in the incubation medium caused 19-fold decrease in AA uptake. The process of AA uptake by MDCK-MDR1 cells appears to be highly sodium-dependent.

3.3. Temperature dependency

Effect of temperature on the uptake of AA by MDCK-MDR1 cells was studied. Initial uptake rates of AA were 15.2 ± 0.62, 7.39 ± 0.30, and 1.88 ± 0.16 pmol/min/mg protein at 37, 25 and 4 °C, respectively. Uptake significantly diminished as incubation temperature was lowered, suggesting that the process is carrier mediated. Uptake rate Ln(v) vs. 1/T was plotted (Fig. 3), and activation energy (E_a) was calculated to be 10.8 kcal/mol.

3.4. pH dependency

Uptake of AA increased with a rise in extracellular pH from 5.0 to 8.5. Relative to pH 7.4, only one fifth of uptake was observed at pH 5.0 (Fig. 4).

3.5. Energy dependency

DNP significantly inhibited the uptake of AA when it was added as a pretreatment or simultaneously during uptake. It caused higher inhibition in the later case. NaN_3 did not show any significant effect in all three conditions as mentioned in the Section 2. Uptake of AA was diminished by 50% with ouabain. However, more effect was noted when cells were pretreated with ouabain (Fig. 5).

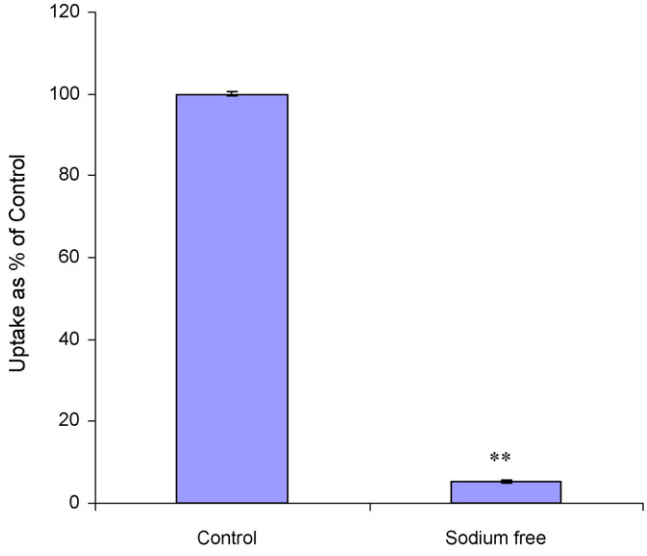

Fig. 2. Effect of Na^+ on [^{14}C]AA uptake in MDCK-MDR1 cells. Uptake of [^{14}C]AA (23.5 μM) was measured in DPBS buffer (pH 7.4) with or without sodium for 30 min. Results are shown as mean ± S.D., n = 4–6. When not shown, error bar is smaller than symbol. $^{**}P < 0.01$.

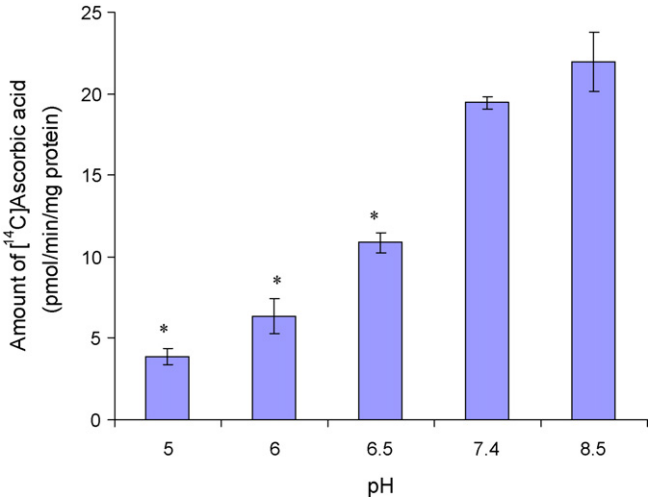

Fig. 4. Effect of pH on [^{14}C]AA uptake in MDCK-MDR1 cells. Uptake of [^{14}C]AA (23.5 μM) was measured in DPBS buffer at different pH values (pH 5.0, 6.0, 6.5, 7.4, 8.5) at 37 °C for 30 min. Results are shown as mean ± S.D., n = 3–6. $^{*}P < 0.05$.

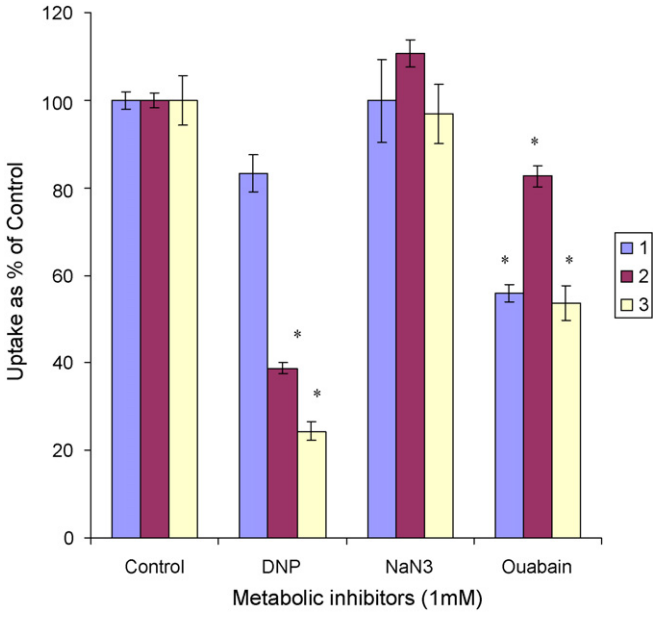

Fig. 5. Effect of metabolic inhibitors on [^{14}C]AA uptake in MDCK-MDR1 cells. Uptake of [^{14}C]AA (23.5 μM) was measured in DPBS buffer (pH 7.4) at 37 °C. (1) Preincubating cells with 1 mM metabolic inhibitors for 30 min; (2) inhibiting the uptake process with 1 mM metabolic inhibitors for 30 min; (3) preincubating cells with 1 mM metabolic inhibitors for 10 min and then inhibiting the uptake process with 1 mM metabolic inhibitors for 30 min. Results are expressed as mean ± S.D., n = 3–6. $^{*}P < 0.05$.

3.6. Concentration dependency

AA uptake was studied as a function of substrate concentration in the range of 5–500 μM. Uptake process was found to be concentration-dependent and saturable at the higher concentrations (Fig. 6). When the kinetic data was plotted in the form of Lineweaver-Burk ($1/v$ vs. $1/[S]$), two separate lines were obtained, which suggested that more than one transporters may exist. The kinetic data was then fit in Eq. (1) separately for the different concentration ranges (5–50 and 50–500 μM) using KaleidaGraph 3.5. The coefficient efficients (R^2) of the fitting were 0.990 and 0.996. The K_m values of SVCT1 and SVCT2 were 83.2 ± 14.0 and 7.27 ± 1.02 μM; and the V_{max} of SVCT1 and SVCT2 were 94.2 ± 4.73 and 44.2 ± 1.99 pmol/min/mg protein, respectively.

3.7. Substrate specificity

[^{14}C]AA uptake was diminished by 90% and 30% with the addition of 1 mM L-AA and D-AA, respectively (Fig. 7). Uptake was reduced to 49%, 67%, and 53% relative to control in the presence of 1 mM DIDS, SITS, and probenecid, respectively. But 1 mM PAHA did not show any effect (Fig. 7).

Effects of mono- and di-substituted benzene derivatives are depicted in Figs. 8 and 9. Among mono-substituted benzene, bromo- and chloro-benzene caused the largest inhibition (56% and 65% relative to control). Nitrobenzene and benzoic acid also produced significant inhibition (36% and 25%). Phenol and benzaldehyde showed no effect. Among di-substituted benzene derivatives, halogen- (Cl, Br, I) and nitro-substituted benzenes significantly lowered AA uptake. We further studied the reversibility of inhibition. Results indicated that the inhibitions induced by AA and most of the substituted benzenes are reversible except 1,4-di-iodo-benzene and 4-iodo-anisole (Fig. 10).

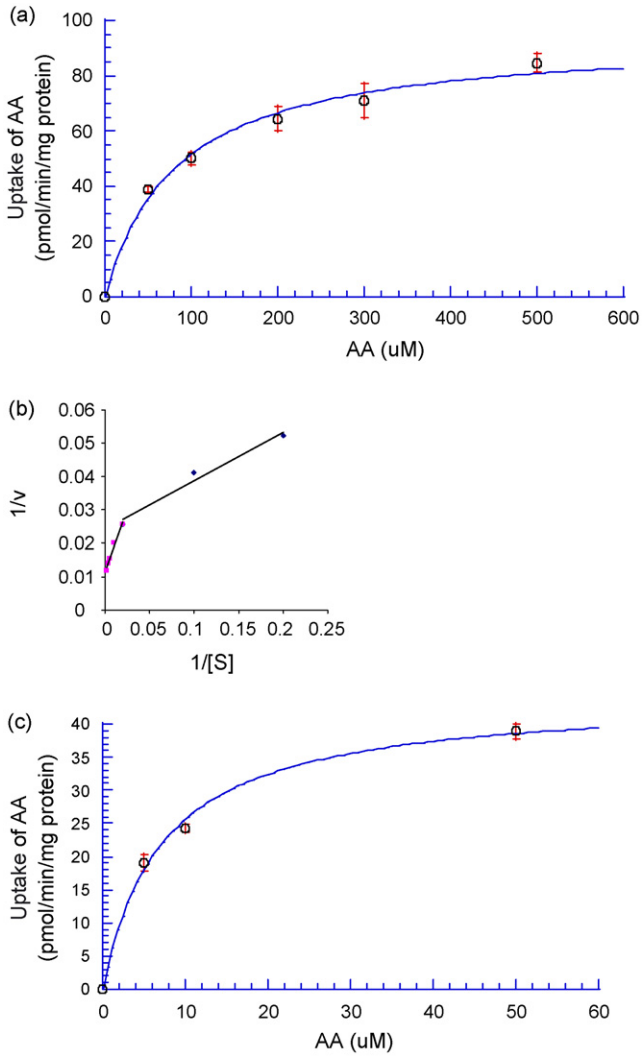

Fig. 6. Saturation kinetics of [^{14}C]AA uptake by MDCK-MDR1 cells. (a) SVCT1: AA (50–500 μM); (c) SVCT2: AA (5–50 μM). (b) Lineweaver-Burk transformation of the data. Cells were incubated at 37 °C in DPBS buffer (pH 7.4) for 30 min in the presence of different concentrations of AA. Results are expressed as mean ± S.D., n = 3–6.

Table 1
Effect of modulators of protein kinase-mediated pathways on AA uptake

	Modulators	Uptake % as of control	Statistics
Control		100 ± 7.19	
Ca/CaM pathway	CaM (50 μM)	60.5 ± 5.84	$P < 0.01$
	KN-62 (10 μM)	81.8 ± 5.65	$P < 0.05$
PKC pathway	PMA (5 μM)	75.6 ± 8.38	$P < 0.01$
PKA pathway	H-89 (25 μM)	93.4 ± 8.56	NS
	Forskolin (100 μM)	97.8 ± 9.66	NS

Uptake of [^{14}C]AA (23.5 μM) was measured in DPBS buffer (pH 7.4) at 37 °C in the absence or presence of different modulators of different protein kinase-mediated pathways. Results are expressed as mean ± S.D., n = 4–6. Statistical comparisons of mean values were evaluated by Student's t-test using GraphPad InStat version 3.1. $P < 0.05$ was considered to be significant. "NS" means not statistically significant.

3.8. Regulation of cellular protein kinase-mediated pathways

The role of different cellular regulation pathways on the process of AA uptake was also investigated. As shown in Table 1, calmidazolium and KN-62, both inhibitors of Ca^{2+}/calmodium (Ca^{2+}/CaM) pathway, caused 40% and 20% inhibition, respectively. PMA, a PKC

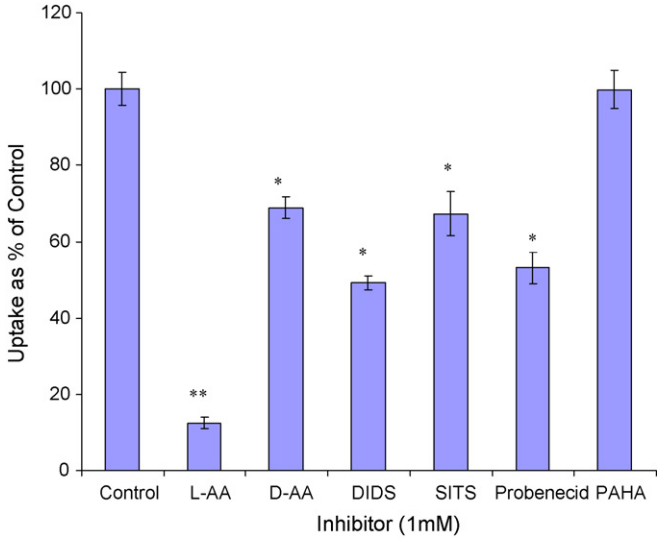

Fig. 7. Effects of unlabelled AA and anion inhibitors on [^{14}C]AA uptake in MDCK-MDR1 cells. Uptake of [^{14}C]AA (23.5 μM) was measured in DPBS buffer (pH 7.4) at 37 °C in the presence of 1 mM inhibitor for 30 min. Results are expressed as mean ± S.D., $n = 3$–6. $^{*}P < 0.05$; $^{**}P < 0.01$.

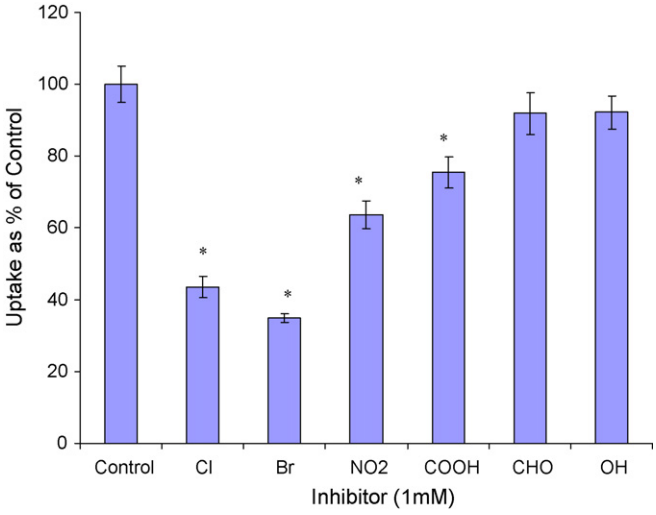

Fig. 8. Effect of various mono-substituted benzene derivatives on [^{14}C]AA uptake in MDCK-MDR1 cells. Uptake of [^{14}C]AA (23.5 μM) was measured in DPBS buffer (pH 7.4) at 37 °C for 30 min in the absence and presence of 1 mM inhibitor. *X*-axis labels stand for the substitute groups of benzene, for example, "Cl" stands for chlorobenzene. Data are expressed as mean ± S.D., $n = 3$–6. $^{*}P < 0.05$.

activator, led to 25% decrease in AA uptake as compare to control. However, no significant effect was observed with H-89 and forskolin, modulators of PKA-mediated pathway.

3.9. Transepithelial transport

We report for the first time transepithelial transport of AA (25.3 μM) across the polarized cell membrane from apical to basal side (A–B) and from basal to apical side (B–A). Cumulative amounts of AA transported over 3 h were 2.16 (A–B) and 1.90 (B–A) nanomoles. Percentages of AA transported relative to donor concentration were 6.1% for A–B and 5.4% for B–A. The permeability values were $8.15 \pm 0.27 \times 10^{-6}$ cm/s for A–B and $7.97 \pm 0.39 \times 10^{-6}$ cm/s for B–A. No significant difference between the permeability of A–B and B–A directions was observed (Fig. 11).

3.10. Confocal imaging

The polarized locations of SVCT1 and SVCT2 in MDCK-MDR1 were observed by confocal microscopy. Z-stack pictures dissect the cell to detect the specific polarized localization of cellular fluorescence. The fluorescence imaging (Fig. 12) indicates that SVCT1 was predominantly located on apical membrane and SVCT2 may be located on both apical and basolateral membranes in MDCK-MDR1 cells.

4. Discussion

AA is an essential cellular nutrient for normal metabolic functions of all mammals. Intestine absorbs AA from exogenous sources (dietary constituents). Kidney handles AA by filtration, excretion,

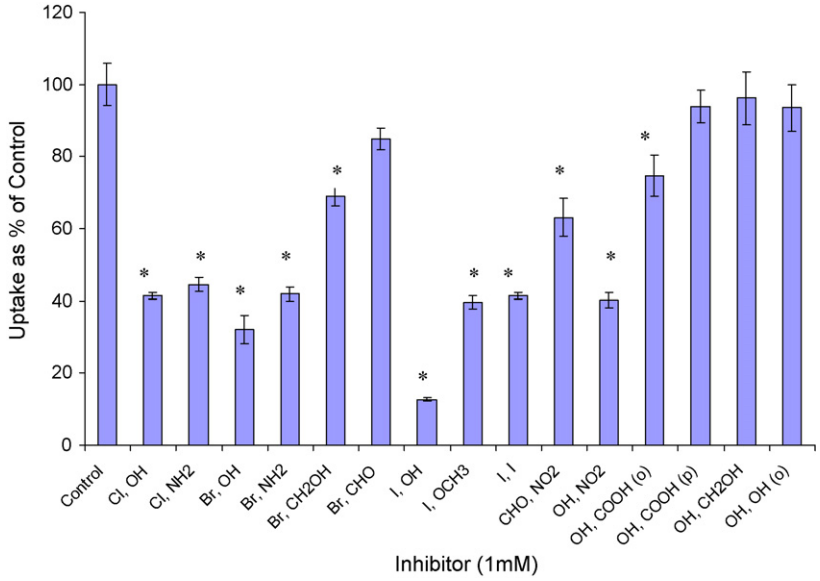

Fig. 9. Effect of various di-substituted benzene derivatives on [^{14}C]AA uptake in MDCK-MDR1 cells. Uptake of [^{14}C]AA (23.5 μM) was measured in DPBS buffer (pH 7.4) at 37 °C for 30 min in the absence and presence of 1 mM inhibitor. *X*-axis labels stand for the *para*-substitute groups of benzene except (*o*) in OH, COOH (*o*) and OH, OH (*o*) for *ortho*-substituted, for example, "Cl, OH" stands for 4-chloro phenol; OH, OH (*o*) stands for *ortho*-phenol. Data is expressed as mean ± S.D., $n = 3$–6. $^{*}P < 0.05$.

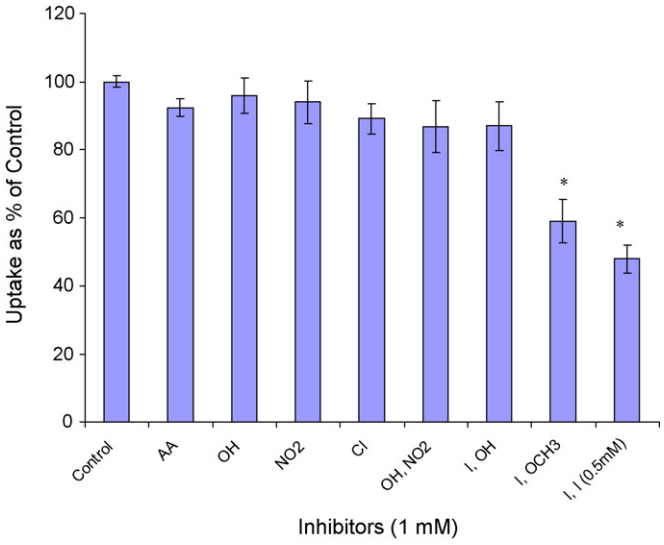

Fig. 10. Reversibility of effect of various inhibitors on [^{14}C]AA uptake in MDCK-MDR1 cells. Uptake of [^{14}C]AA (23.5 μM) was measured in DPBS buffer (pH 7.4) at 37 °C for 30 min after preincubating the cells with various inhibitors for 1 h and then washing off inhibitors with DPBS buffer before adding [^{14}C]AA. The concentration of all inhibitors is 1 mM except that of 1,4-di-iodo-benzene is 0.5 mM due to its solubility. *X*-axis labels stand for the substitute groups of benzene except AA for L-AA. Data are expressed as mean ± S.D., $n = 3–6$. $^{*}P < 0.05$.

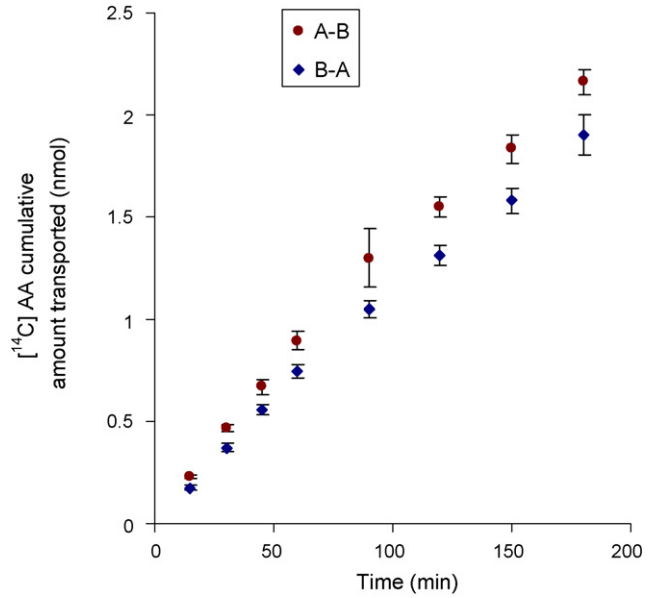

Fig. 11. Transepithelial transport of [^{14}C]AA in MDCK-MDR1 cells. Cumulative amount of transported [^{14}C]AA (23.5 μM) was calculated according to Eq. (2). Samples (100 μL) were taken at predetermined time intervals (15, 30, 45, 60, 90, 120, 150, 180 min) and then analyzed by scintillation counter. Results are expressed as mean ± S.D., $n = 3–6$.

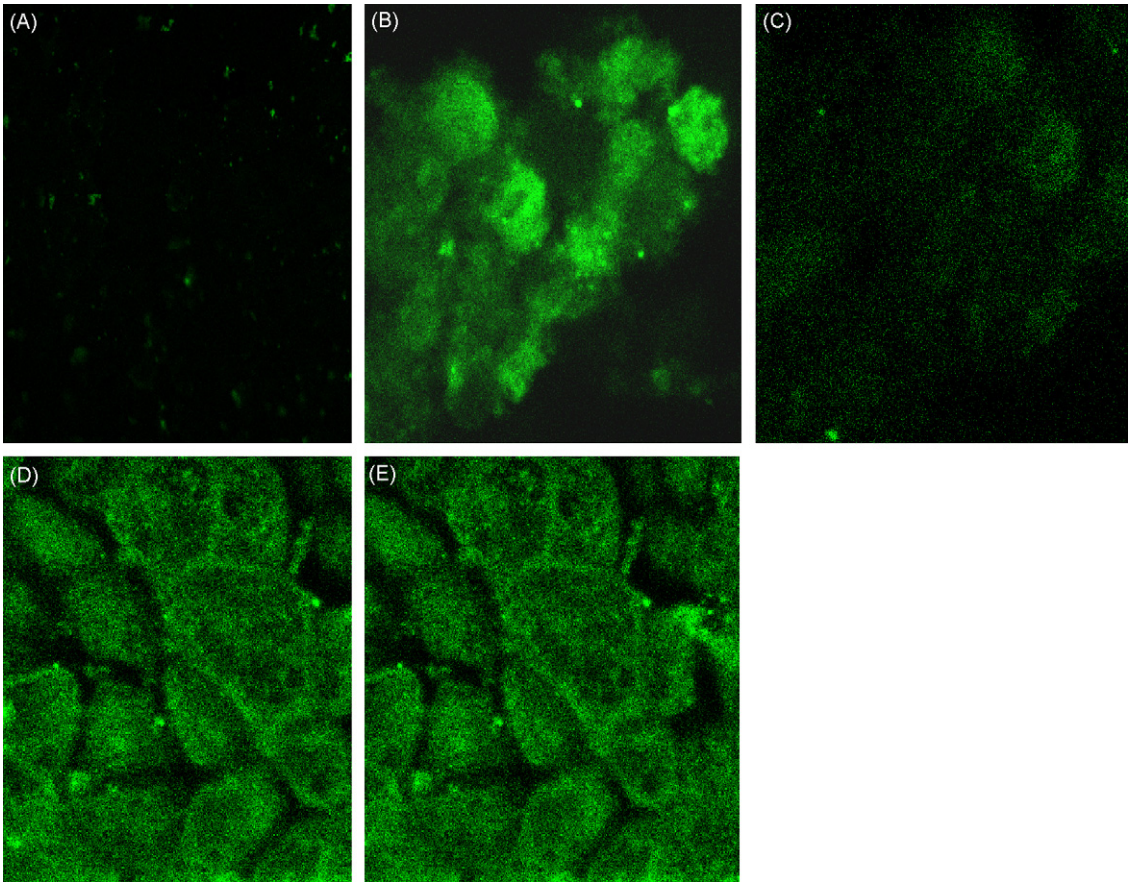

Fig. 12. Confocal imaging of SVCT1 and SVCT2 in MDCK-MDR1 cells. (A) No fluorescence in the negative control containing no primary antibodies but goat serum only; (B) SVCT1: fluorescence picture was captured from the top surface (apical surface) indicating the localization of SVCT1 on the apical membrane of MDCK cells; (C) SVCT1: fluorescence picture was captured from the bottom showing no fluorescence implying no localization of SVCT1 in the basolateral membrane of MDCK cells. (D) SVCT2 (picture from the top surface); (E) SVCT2 (picture from the bottom surface). Both these pictures show similar fluorescence intensity suggesting SVCT2 either present on the basolateral membrane or both apical and basolateral membranes of MDCK cells.

and reabsorption, which is essential to make up urinary loss. It maintains the balanced plasma level of AA in the body. MDCK-MDR1 cells are canine kidney cells transfected with human MDR1 genes. It has been used as an *in vitro* model to study the permeability of nutrient conjugated prodrugs of saquinavir (Jain et al., 2005; Luo et al., 2006). Recently, polarized expression of SVCT1 in Caco-2 cells and MDCK cells was reported (Boyer et al., 2005; Maulen et al., 2003; Subramanian et al., 2004). In this work, we investigated the mechanisms involved in the uptake and transport of AA and substrate specificity of SVCT in MDCK-MDR1 cells. We studied the effect of a series of mono- and di-substituted benzene derivatives to the uptake of AA. Results of this work may be used to evaluate the feasibility of using MDCK-MDR1 cell line as an *in vitro* model to study the permeability of AA conjugated prodrugs. The properties of AA uptake may be compared with that of vitamin B uptake in MDCK-MDR1 cells for the selection of transporters to be targeted for drug delivery.

Time course of AA uptake exhibits a linear increase in uptake till 90 min (Fig. 1), indicating that SVCT is a high capacity transporter. Uptake of AA was found to be strongly dependent on the presence of Na^+ in the incubation medium, suggesting a Na^+-dependent transport mechanism for AA (Fig. 2). Temperature-dependent uptake of AA by MDCK-MDR1 cells is strongly evident (Fig. 3). Activation energy (E_a) of AA uptake is two times as that of vitamin B uptake by MDCK-MDR1 cells (Luo et al., 2006), which means the process of active vitamin C uptake requires more energy compared to that of vitamin B.

Amount of AA uptake is enhanced as pH increased (Fig. 4). The pK_{a1} of AA is 4.17. Therefore, it primarily exists in the form of ascorbate (−1 charge) above pH 5.0, which means pH dependency is not due to the ionic state of AA. On the other hand, the effect of pH may suggest that SVCT has higher affinity with ascorbate at higher pH (Liang et al., 2001; Tsukaguchi et al., 1999). This phenomenon is different from sodium-dependent multi-vitamin transport (SMVT), in which pH affects the ionic fraction of biotin (Luo et al., 2006). SVCT has high affinity with the ionized form of AA, which suggests that the ion–ion and/or ion–polarity interactions between SVCT and its substrates are predominant driving forces for the binding of SVCT. Lower pH may cause protonation of histidine residues in SVCT and thus reduce the binding affinity of SVCT with its substrates (Liang et al., 2001).

Unlabelled AA (both L- and D-isomers) caused significant inhibition to [^{14}C]AA uptake (Fig. 7). About 3-fold higher inhibition with L-AA as compared to D-AA suggests higher specificity of the transporter for L-isomer. AA exists as an anion (ascorbate) under experimental condition (pH 7.4). Uptake was performed in the presence of various anion inhibitors such as DIDS, SITS, probenecid, and PAHA. All the inhibitors examined except PAHA caused significant inhibition (Fig. 7). Inhibition of ascorbate uptake by anions has also been reported in other cells (Dixon et al., 1991). These results indicate that certain anions may affect the interaction of SVCT with ascorbate and the location of the transport system could be the plasma membrane.

DNP and ouabain produced significant inhibitions of AA uptake (Fig. 5). DNP functions more likely as a structural inhibitor than an energy inhibitor since it simultaneously competes with AA. Ouabain acts more as an energy inhibitor that blocks the Na^+–K^+–ATP pathway. The results of DNP inhibition to AA uptake indicate that substituted benzene derivatives may affect the uptake of AA. Structure of DNP and ouabain is somewhat similar to that of AA as both contain a five- or six-membered ring and a double bond conjugated with an oxygen anion, which raises a question whether substituted benzene affects AA uptake. To answer this question, we further studied the effect of a series of mono- and di-substituted benzene derivatives on the uptake of AA. The process significantly decreased in the presence of electron-withdrawing groups such as halogen- and nitro-substituted benzenes (Figs. 8 and 9). Inhibition by unlabelled AA and most of the substituted benzenes was reversible except di-iodo-benzene and iodo-substituted anisole (Fig. 10). The effects of halogen-substituted benzenes, 6-deoxy-AA and diclofenamic acid indicate that the halogen elements may facilitate the interaction of SVCT with its substrates. If a drug contains halogen-substituted benzene as part of its structure, i.e., diclofenamic acid, it may interfere with the uptake of AA. One possibility is the structural similarity between substituted benzene and AA such as a negatively charged ring conjugated with an electron-withdrawing atom. Halogen- and nitro-benzenes may be recognized by SVCT. Another possibility is that these substituted benzenes are prone to generating free radicals thus inhibiting AA uptake. Further studies are needed to elucidate the mechanism. Investigation on structural requirements for the binding of SVCT with its substrates might be difficult due to the lack of 3D structure of SVCT at this time.

AA uptake by MDCK-MDR1 cells was found to be concentration-dependent and saturable in the micromolar range with a K_m of 83.2 and 7.27 μM for SVCT1 and SVCT2, respectively (Fig. 6). The K_m value (83.2 μM) of SVCT1 obtained here in MDCK-MDR1 cells was less than that (125 μM) in Caco-2 cells (Maulen et al., 2003), which indicates that the affinity of SVCT1 in kidney cells is higher than that in intestinal cells. The K_m value (7.27 μM) of SVCT2 in MDCK-MDR1 cells was comparable with that (8 μM) in Caco-2 cells (Maulen et al., 2003). Affinity of SVCT with vitamin C is lower than that of SMVT with vitamin B (K_m of 13.0 μM) while capacity of SVCT is higher than that of SMVT in MDCK-MDR1 cells. AA transports in both A–B and B–A directions with similar permeability in MDCK-MDR1 cells (Fig. 11). P_{A-B} value of AA is about 50% higher than that of vitamin B while P_{B-A} value of AA is about 300% higher in MDCK-MDR1 cells (Luo et al., 2006). The relative values of kinetic permeability parameters may explain the facts that the plasma concentration of AA and its re-absorption by kidney is much higher than that of vitamin B. The results of confocal imaging suggest that SVCT1 is mainly expressed on the apical membrane and SVCT2 may be located on both apical and basal membranes in MDCK-MDR1 cells. Similar results have also been reported in Caco-2 and MDCK cells by Boyer et al. (2005).

Several inter and intra cellular stimuli (hormones, paracrine factors, signaling molecules, etc.) are involved in the regulation of expression sodium-ascorbate cotransporters (Wilson, 2005). Analysis of deduced primary amino acid sequence of hSVCT1 and hSVCT2 indicated the presence of five putative PKC phosphorylation sites and hSVCT1 having an additional PKA site (Liang et al., 2001). Also, it has been demonstrated that the uptake of vitamin C mediated by hSVCTs expressed in COS-1 cells was under the regulation of PKC-mediated pathway (Liang et al., 2002). We also investigated the regulation of AA uptake by the intracellular protein kinase-mediated pathways (Table 1). Calmidazolium and KN-62 caused a significant inhibition suggesting that the uptake process is under the regulation of Ca^{2+}/CaM mediated pathway. Pretreatment of PMA led to a significant decrease in AA uptake, indicating the role of PKC-mediated pathway on the regulation of AA uptake. On the other hand, the role for PKA-mediated pathway was not evident as indicated by the lack of significant effect on AA uptake by H-89 and forskolin treated cells.

In conclusion, this study demonstrated for the first time functional evidence of a sodium-dependent vitamin C transporter, SVCT, in MDCK-MDR1 cells. A series of electrophile-substituted benzene derivatives were recognized by SVCT, which may challenge the concept that SVCT is specific only for AA and its analogues.

AA uptake is regulated by both protein kinase C and Ca^{2+}/CaM mediated pathways. Bidirectional transport of AA in kidney cells indicates a significant role of kidney in AA reabsorption and excretion. MDCK-MDR1 cell line may be utilized as a valuable *in vitro* tool for screening the permeability characteristics of AA conjugated prodrugs.

Acknowledgement

Authors acknowledge Tim Quinn, School of Medicine, UMKC for confocal microscopic imaging. This study was supported by NIH grant R01 AI 071199.

References

Astuya, A., Caprile, T., Castro, M., Salazar, K., Garcia, M.L., Reinicke, K., Rodriguez, F., Vera, J.C., Millan, C., Ulloa, V., Low, M., Martinez, F., Nualart, F., 2005. Vitamin C uptake and recycling among normal and tumor cells from the central nervous system. J. Neurosci. Res. 79, 146–156.

Bowers-Komro, D.M., McCormick, D.B., 1991. Characterization of ascorbic acid uptake by isolated rat kidney cells. J. Nutr. 121, 57–64.

Boyer, J.C., Campbell, C.E., Sigurdson, W.J., Kuo, S.M., 2005. Polarized localization of vitamin C transporters, SVCT1 and SVCT2, in epithelial cells. Biochem. Biophys. Res. Commun. 334, 150–156.

Castro, M., Caprile, T., Astuya, A., Millan, C., Reinicke, K., Vera, J.C., Vasquez, O., Aguayo, L.G., Nualart, F., 2001. High-affinity sodium-vitamin C co-transporters (SVCT) expression in embryonic mouse neurons. J. Neurochem. 78, 815–823.

Dalpiaz, A., Pavan, B., Scaglianti, M., Vitali, F., Bortolotti, F., Biondi, C., Scatturin, A., Tanganelli, S., Ferraro, L., Prasad, P., Manfredini, S., 2004. Transporter-mediated effects of diclofenamic acid and its ascorbyl pro-drug in the in vivo neurotropic activity of ascorbyl nipecotic acid conjugate. J. Pharm. Sci. 93, 78–85.

Dalpiaz, A., Pavan, B., Vertuani, S., Vitali, F., Scaglianti, M., Bortolotti, F., Biondi, C., Scatturin, A., Tanganelli, S., Ferraro, L., Marzola, G., Prasad, P., Manfredini, S., 2005a. Ascorbic and 6-Br-ascorbic acid conjugates as a tool to increase the therapeutic effects of potentially central active drugs. Eur. J. Pharm. Sci. 24, 259–269.

Dalpiaz, A., Pavan, B., Scaglianti, M., Vitali, F., Bortolotti, F., Biondi, C., Scatturin, A., Manfredini, S., 2005b. Vitamin C and 6-amino-vitamin C conjugates of diclofenac: synthesis and evaluation. Int. J. Pharm. 291, 171–181.

Daruwala, R., Song, J., Koh, W.S., Rumsey, S.C., Levine, M., 1999. Cloning and functional characterization of the human sodium-dependent vitamin C transporters hSVCT1 and hSVCT2. FEBS Lett. 460, 480–484.

Dixon, S.J., Kulaga, A., Jaworski, E.M., Wilson, J.X., 1991. Ascorbate uptake by ROS 17/2.8 Osteoblast-like cells: substrate specificity and sensitivity to transport inhibitors. J. Bone Miner. Res. 6, 623–629.

Garland, D.L., 1991. Ascorbic acid and the eye. Am. J. Clin. Nutr. 54, 1198S–1202S.

Jain, R., Agarwal, S., Majumdar, S., Zhu, X., Pal, D., Mitra, A.K., 2005. Evasion of P-gp mediated cellular efflux and permeability enhancement of HIV-protease inhibitor saquinavir by prodrug modification. Int. J. Pharm. 303, 8–19.

Liang, W.J., Johnson, D., Jarvis, S.M., 2001. Vitamin C transport systems of mammalian cells. Mol. Membr. Biol. 18, 87–95.

Liang, W.J., Johnson, D., Ma, L.S., Jarvis, S.M., 2002. Regulation of the human vitamin C transporters expressed in COS-1 cells by protein kinase C. Am. J. Physiol. Cell Physiol. 283, C1696–C1704.

Luo, S., Kansara, V.S., Zhu, X., Mandava, N.K., Pal, D., Mitra, A.K., 2006. Functional characterization of sodium-dependent multivitamin transporter in MDCK-MDR1 cells and its utilization as a target for drug delivery. Mol. Pharm. 3, 329–339.

Manfredini, S., Vertuani, S., Pavan, B., Vitali, F., Scaglianti, M., Bortolotti, F., Biondi, C., Scatturin, A., Prasad, P., Dalpiaz, A., 2004. Design, synthesis and in vitro evaluation on HRPE cells of ascorbic and 6-bromoascorbic acid conjugates with neuroactive molecules. Bioorg. Med. Chem. 12, 5453–5463.

Maulen, N.P., Henriquez, E.A., Kempe, S., Carcamo, J.G., Schmid-Kotsas, A., Bachem, M., Grunert, A., Bustamante, M.E., Nualart, F., Vera, J.C., 2003. Up-regulation and polarized expression of the sodium-ascorbic acid transporter SVCT1 in post-confluent differentiated CaCo-2 cells. J. Biol. Chem. 278, 9035–9041.

Padh, H., Aleo, J.J., 1987. Characterization of the ascorbic acid transport by 3T6 fibroblasts. Biochim. Biophys. Acta 901, 283–290.

Park, J.B., Levine, M., 2000. Intracellular accumulation of ascorbic acid is inhibited by flavonoids via blocking of dehydroascorbic acid and ascorbic acid uptakes in HL-60, U937 and Jurkat cells. J. Nutr. 130, 1297–1302.

Rose, R.C., 1986. Ascorbic acid transport in mammalian kidney. Am. J. Physiol. 250, F627–F632.

Rose, R.C., 1988. Transport of ascorbic acid and other water-soluble vitamins. Biochim. Biophys. Acta 947, 335–366.

Rumsey, S.C., Welch, R.W., Garraffo, H.M., Ge, P., Lu, S.F., Crossman, A.T., Kirk, K.L., Levine, M., 1999. Specificity of ascorbate analogs for ascorbate transport. Synthesis and detection of [(125)I]6-deoxy-6-iodo-L-ascorbic acid and characterization of its ascorbate-specific transport properties. J. Biol. Chem. 274, 23215–23222.

Said, H.M., Mohammed, Z.M., 2006. Intestinal absorption of water-soluble vitamins: an update. Curr. Opin. Gastroenterol. 22, 140–146.

Subramanian, V.S., Marchant, J.S., Boulware, M.J., Said, H.M., 2004. A C-terminal region dictates the apical plasma membrane targeting of the human sodium-dependent vitamin C transporter-1 in polarized epithelia. J. Biol. Chem. 279, 27719–27728.

Talluri, R.S., Katragadda, S., Pal, D., Mitra, A.K., 2006. Mechanism of L-ascorbic acid uptake by rabbit corneal epithelial cells: evidence for the involvement of sodium-dependent vitamin C transporter 2. Curr. Eye Res. 31, 481–489.

Tang, F., Horie, K., Borchardt, R.T., 2002. Are MDCK cells transfected with the human MDR1 gene a good model of the human intestinal mucosa? Pharm. Res. 19, 765–772.

Tsukaguchi, H., Tokui, T., Mackenzie, B., Berger, U.V., Chen, X.Z., Wang, Y., Brubaker, R.F., Hediger, M.A., 1999. A family of mammalian Na^+-dependent L-ascorbic acid transporters. Nature 399, 70–75.

Wang, H., Dutta, B., Huang, W., Devoe, L.D., Leibach, F.H., Ganapathy, V., Prasad, P.D., 1999. Human Na(+)-dependent vitamin C transporter 1 (hSVCT1): primary structure, functional characteristics and evidence for a non-functional splice variant. Biochim. Biophys. Acta 1461, 1–9.

Wilson, J.X., 2005. Regulation of vitamin C transport. Annu. Rev. Nutr. 25, 105–125.